NICKEL TETRASULPHONATED PHTHALOCYANINE (NiTsPc) NANOSTRUCTURES VIA POLYCARBONATE MEMBRANE: ENHANCEMENT ON OPTICAL, MORPHOLOGICAL AND ELECTRICAL PROPERTIES

MIRZA MOHD FAWWAZ BIN FAIZAN BEG

DEPARTMENT OF PHYSICS
FACULTY OF SCIENCE
UNIVERSITY OF MALAYA
KUALA LUMPUR
2015

NICKEL TETRASULPHONATED PHTHALOCYANINE (NiTsPc) NANOSTRUCTURES VIA POLYCARBONATE MEMBRANE: ENHANCEMENT ON OPTICAL, MORPHOLOGICAL AND ELECTRICAL PROPERTIES

MIRZA MOHD FAWWAZ BIN FAIZAN BEG

RESEARCH REPORT SUBMITTED IN FULFILLMENT OF THE REQUIREMENTS FOR THE DEGREE OF MASTER OF SCIENCE

(APPLIED PHYSICS)

DEPARTMENT OF PHYSICS
FACULTY OF SCIENCE
UNIVERSITY OF MALAYA
KUALA LUMPUR

UNIVERSITI MALAYA

ORIGINAL LITERARY WORK DECLARATION

Name of candidate: Mirza Mohd Fawwaz Bin Faizan Beg (I.C: 870519-56-5657)

Registration/Matric No: SGB130002

Name of Degree: Master of Degree of Applied Physics

Title of Dissertation: Nickel Tetrasulphonated Phthalocyanine (NiTsPc) Nanostructures via Polycarbonate Membrane: Enhancement on Optical, Morphological and Electrical Properties

Field of Study: Nanomaterials

I do solemnly and sincerely declare that:

(1) I am the sole author/writer of this work;

(2) This work is original;

(3) Any use of any work in which copyright exists was done by way of fair dealing and for permitted purposes and any excerpt or extract from, or reference to or reproduction of any copyright work has been acknowledged in this work;

(4) I do not have any actual knowledge nor ought I reasonably to know that the making of this work constitutes an infringement of any copyright work;

(5) I hereby assign all and every rights in the copyright to this work to the University of Malaya ("UM"), who henceforth shall be owner of the copyright in this work and that any reproduction or use in any form or by any means whatsoever is prohibited without the written consent of UM having been first had and obtained;

(6) I am fully aware that if in the course of making this Work I have infringed any copyright whether intentionally or otherwise. I may be subject to legal action or any other action as may be determined by UM.

Candidate's Signature Date

Subscribed and solemnly declared before,

Witness' Signature Date

Name:

Designation:

UNIVERSITI MALAYA

PERAKUAN KEASLIAN PENULISAN

Nama: Mirza Mohd Fawwaz Bin Faizan Beg (NO. K.P: 870519-56-5657)

No. Pendaftaran: SGB130002

Nama Ijazah: Ijazah Sarjana Fizik Gunaan

Tajuk Disertasi: Nickel Tetrasulphonated Phthalocyanine (NiTsPc) Nanostructures via Polycarbonate Membrane: Enhancement on Optical, Morphological and Electrical Properties

Bidang Penyelidikan: Nanobahan

Saya dengan sesungguhnya dan sebenarnya mengaku bahawa

(1) Saya adalah satu-satunya pengarang /penulis hasil kerja ini;
(2) Hasil kerja ini adalah asli;
(3) Apa-apa penggunaan mana-mana hasil kerja yang mengandungi hakcipta telah dilakukan secara urusan yang wajar dan bagi maksud yang dibenarkan dan apa-apa petikan, ekstrak, rujukan atau pengeluaran semula daripada atau kepada mana-mana hasil kerja yang mengandungi hakcipta telah dinyatakan dengan sejelasnya dan secukupnya dan satu pengiktirafan tajuk hasil kerja tersebut dan pengarang/penulisnya telah dilakukan di dalam hasil kerja ini;
(4) Saya tidak mempunyai apa-apa pengetahuan sebenar atau patut semunasabahnya tahu bahawa penghasilan hasil kerja ini melanggar suatu hakcipta hasil kerja yang lain;
(5) Saya dengan ini menyerahkan kesemua dan tiap-tiap hak yang terkandung di dalam hakcipta hasil Kerja ini kepada Universiti Malaya ("UM") yang seterusnya mula dari sekarang adalah tuan punya kepada hakcipta di dalam hasil kerja ini dan apa-apa pengeluaran semula atau penggunaan dalam apa jua bentuk atau dengan apa juga cara sekalipun adalah dilarang tanpa terlebih dahulu mendapat kebenaran bertulis dari UM.
(6) Saya sedar sepenuhnya sekiranya dalam masa penghasilan hasil kerja ini saya telah melanggar suatu hakcipta hasil kerja yang lain sama ada dengan niat atau sebaliknya, saya boleh dikenakan tindakan undang-undang atau apa-apa tindakan lain sebagaimana yang diputuskan oleh UM.

Tandatangan Calon Tarikh

Di perbuat dan sesungguhnya diakui di hadapan,

Tandatangan Saksi Tarikh

Nama:

Jawatan:

ABSTRACT

Nickel tetrasulfonated phthalocyanine (NiTsPc) with planar aromatic structures is an ideal building block for organic nanostructures. NiTsPc can self-assemble into stacks through π–π interaction, exhibit high thermal and chemical stabilities, and possess outstanding electrical and optical properties. In this paper, the optical, morphological and electrical properties of NiTsPc nanostructures were investigated. NiTsPc nanostructures were synthesized via polycarbonate membrane of immersion technique. The polycarbonate membrane was immersed in NiTsPc solution for 1 hour and 24 hours. Different annealing temperatures of 50 °C and 100 °C were applied prior to the dissolution of polycarbonate membranes. NiTsPc nanostructures were characterised by UV-Vis spectroscopy, Raman spectroscopy, photoluminescence spectroscopy, field emission scanning electron microscopy and four point probes.

ABSTRAK

Nickel tetrasulfonated phthalocyanines (NiTsPc) dengan struktur satah vilectron adalah susunan blok yang ideal untuk nanostruktur vilectro. Nanostruktur ini boleh membesar sendiri ke dalam susunan melaui interaksi π–π, mempamerkan termal yang tinggi dan penstabilan kimia dan mempunyai sifat elektrik dan optikal yang hebat. Dalam kajian ini, sifat optikal, morfologi dan elektrik bahan NiTsPc disiasat. Nanostruktur NiTsPc di sediakan melalui teknik rendaman polikarbonat membran. Membran polikarbonat direndamkan dalam larutan NiTsPc selama 1 jam dan 24 jam. Perbezaan suhu penyepuhlindapan pada 50 °C dan 100 °C di gunakan sebelum pembubaran pada polikarbonat membran. NiTsPc nanostruktur dianalisis menggunakan spektroskopi UV-Vis, spektroskopi Raman, spektroskopi fotoluminas, mikroskopi bidang pembebasan pengimbasan vilectron dan kuar empat mata.

ACKNOWLEDGEMENT

In the Name of Allah, the Most Beneficent,the Most Merciful

I would like to express my great gratitude to my supervisor, Dr.Azzuliani Binti Supangat, for her constructive recommendations and suggestions during this study. Her constant encouragement, guidance, patience and invaluable instruction that contributed to the fulfilment of this work and my academic life throughout my research programme very much appreciated.

I would also like to express my sincere appreciation to the staff and students at the Low Dimensional Materials Research Centre for their support and their assistance in manufacturing various devices and repairing instruments. Thanks are due to all the members of the staff at UITM Puncak Alam, Shah Alam for their friendly support and help all rounds especially for FESEM analysis.

I am extremely grateful to Muhamad Saipul Fakir and Nor Asmaliza Bakar for the extensive help in teaching me on how to use instruments for characterization. I am also grateful to Mohd Arif and Maisara for the extensive help with Surface Profilometer. Sincere gratitude to Siti Hajar and Mohd Shahino for help with the use of the Four Point Probe.

Huge thanks are given to my beloved family, Pn. Nurul Farehan Ismail and Pn. Azyan Fahruddin for their continuous support, understanding, encouragement and blessings; you'll never know how much your support has meant to me.

TABLE OF CONTENTS

LIST OF FIGURES

LIST OF TABLES

LIST OF SYMBOLS AND ABBREVIATIONS

NiTsPc	Nickel Tetrasulfonated Phthalocyanine
NiPc	Nickel Phthalocyanine
Pc	Phthalocyanines
MPcs	Metal Phthalocyanines
HOMO	Highest Occupied Molecular Orbital
LUMO	Lowest Unoccupied Molecular Orbital
eV	Electronvolt
°C	Centigrade
I	Current
V	Voltage
R	Resistance
RR	Rectification Ratio
SCLC	Space Charge Limited Current
C	Capacitance
F	Frequency
K_4NiTSPc	Nickel (II) 4,4', 4", 4"'potassium tetrasulphophthalocyanine
AC	Alternating Current
DC	Direct Current
KrF	KriptonFlouride
ITO	Indium Tin Oxide
LbL	Layer by layer
DODAB	Dioctadecyl Dimethylammonium Bromide
UV	Ultraviolet
Vis	Visible
NIR	Near infrared
CCD	Charge Coupled Device

nm	nanometer
µm	micrometer
PL	Photoluminescence
M4PPs	Microscopic four-point probes
FESEM	Field Emission Scanning Electron Microscopy
T	Thickness
G	Geometric factor
Ω	Ohm
ρ	Resistivity
σ	Conductivity

CHAPTER 1: INTRODUCTION

1.1: Phthalocyanine

In recent years organic semiconducting materials are rapidly making an impact in the area of electronics and optoelectronics. Phthalocyanines (Pcs) with planar aromatic structures are ideal building blocks for organic nanostructures. They can self-assemble into stacks through π–π interaction [1], exhibit high thermal and chemical stabilities, and possess outstanding electrical and optical properties. Metal Phthalocyanines (MPcs) are a family of medium sized organic molecules that have broad applications in fields including non-linear optics, molecular electronics, and fabrication of electrochemical sensors [2]. The utility of these complex molecules derives from their attractive properties, including high chemical, thermal, and mechanical stability [3-5]. In recent years, organic materials have become increasingly important in the field of optoelectronics due to their various applications. The molecular structure of Pcs and MPcs can be seen in Fig. 1 and Fig. 2. Phthalocyanines as a class of organic materials are chemically and thermally stable and can be easily deposited as thin films with high quality by thermal evaporation without dissociation. One of the major advantages of using Pcs is their chemical stability as well as the ability to readily modify the molecular structure allowing the molecular engineering of their physical properties accordingly.

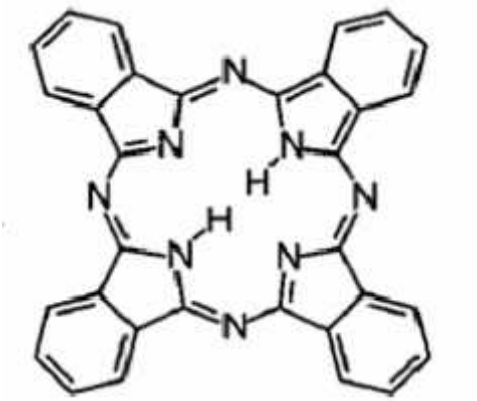

Fig. 1: Molecular structure of phthalocyanines

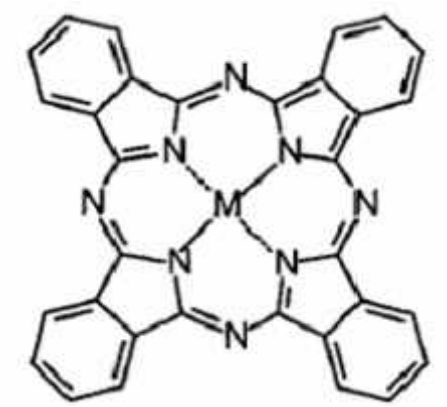

Fig. 2: Molecular structure of metal phthalocyanines

In this context, phthalocyanine (Pc) molecules are particularly appealing because of their unique optical and electrical properties. In general, they can be classified as p-type semiconductors characterized by low mobility and low carrier concentration [6]. Phthalocyanine represents a large family of heterocyclic conjugated molecules, consisting of four benzoisoindole units, with potential applications in the fabrication of solar cells, chemical sensors, electronic displays and optical data storage systems [7-10]. The electronic structure of MPc can be characterized by delocalization of the electrons with highest occupied molecular orbital (HOMO), lowest unoccupied molecular orbital (LUMO) transitions in the visible region and are important optical and semiconducting materials for electronics and optoelectronics device. The parameters of MPc thin films depend on a variety of parameters including metal atoms in centre, conjugated structure and substitutional groups. The electrical and optical properties of thin films are strongly affected by chemical substitutions at the molecular ligand [11-14]. Therefore, Pcs are one of the most stable and photosensitive organic semiconductor and for a long time have been widely used for the creation of photo-converters and solar cells as p-type components [13, 15-18]. Phthalocyanine and metal phthalocyanine have band gap below 1.8 eV, have been widely used in p-type semiconductor layers in organic solar cells in the form of bi-layer structures [19, 20]. Phthalocyanines also are

one of the most useful heterocyclic materials. There are still many investigations on their technological applications in different scientific areas such as chemical sensors [21, 22], solar cells [23], semiconductors [24] and catalyst [25]. Phthalocyanines and their metal complex derivatives have strong delocalized 18 π-electronic structures, good thermal stability and interesting visible area optical properties.

The hydrogen atoms of the central cavity can be replaced by more than 70 elements, almost every metal, and also some metalloids. A great number of unique properties arise from this electronic delocalization, which makes these compounds applicable in different fields of materials science. Thus, phthalocyanines are thermally and chemically stable. They can be heated up to 500 °C under high vacuum without decomposition and remain unaltered when exposed to the action of non-oxidative acids or bases. But the most remarkable feature that makes these molecules play an exceptional role in the area of materials science is their versatility. The coordination number of the square-planar phthalocyanine is four. Thus, according to the size and oxidation state of the metal, one or even two can be included into the phthalocyanine core. The inclusion of different metals allows the tuning of the physical properties that these compounds exhibit. A summary of some applications of phthalocyanine are illustrated in Figure 3.

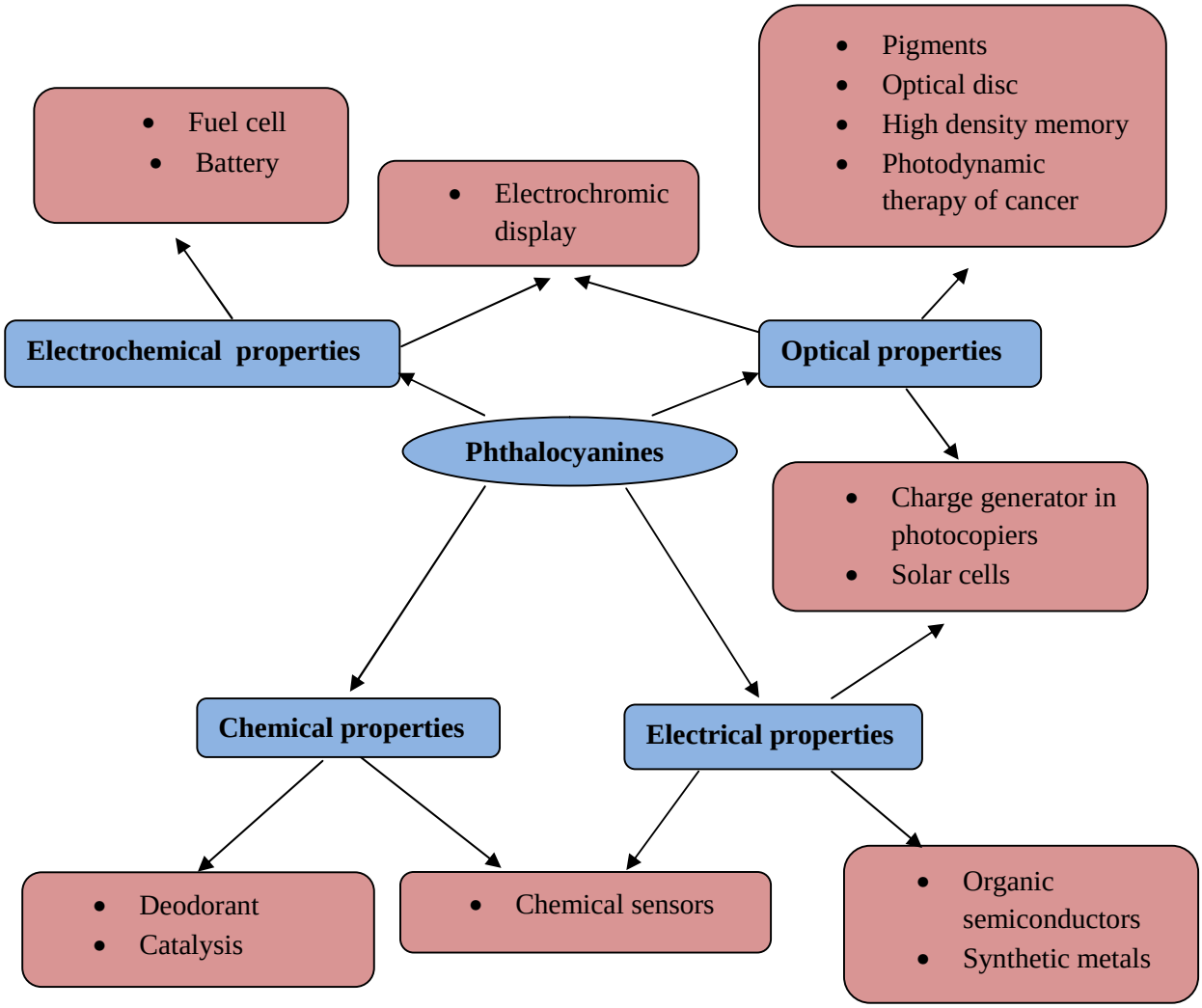

Fig. 3: Applications of phthalocyanine

1.2: Aim of the work

In the present work, the optical, morphological and electrical properties of nickel tetrasulfonatedphthalocyanine (NiTsPc) nanostructures were investigated. NiTsPc nanostructures were synthesised via polycarbonate membrane of immersion techniques.

CHAPTER 2: LITERATURE REVIEW

2.1 Metal phthalocyanine

Nickel phthalocyanine (NiPc) is one of the metal phthalocyanine families, which has shown good sensing and electronic properties [26-29]. Jacob et al. have reported that the NiPc nanostructures can be synthesised by employing an ionic liquid media [30]. In addition, the electrical properties of NiPc in surface type cells have shown the potential for electronic applications [31-33]. Ahmad et al. have investigated the NiPc derivative, nickel tetrasulphonatedphthlocyanines (NiTsPc) for temperature sensor applications, which indicated the enhancement of the electrical properties of NiPc by attaching a tetrasulfonic functional group [34]. The molecular structure of NiPc and NiTsPc are shown in Fig. 4 and Fig. 5.

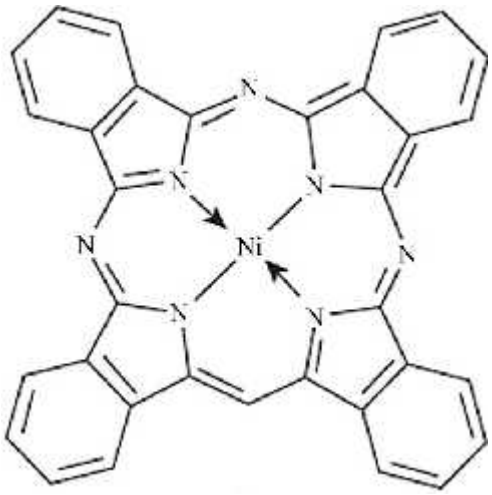

Fig. 4: The molecular structure of NiPc

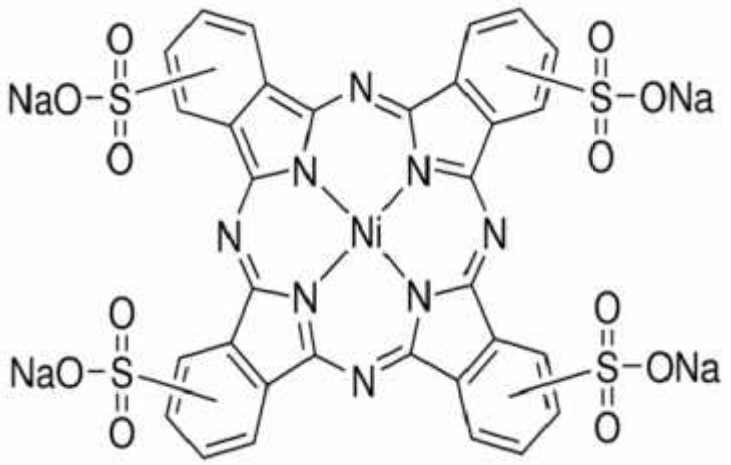

Fig. 5: The molecular structure of NiTsPc

A p-type NiPc thin film has shown a significantly higher mobility of 7×10^{-5} m^2 V^{-1} s^{-1} if compared with the carrier mobility of other metal phthalocyanine [35]. Due to the higher carrier mobility of NiPc, it is an attractive candidate for the efficient organic photovoltaic cells since transport of optically excited carriers to their respective electrodes is expected to be much faster, thus reducing carrier recombination and subsequently increasing power conversion efficiency of the device. Anthopoulos and Shafai [36] have fabricated multilayer sandwich structures of Au/NiPc/Pb. The current–voltage (*I–V*) measurements under forward bias show ohmic conduction in the lower voltage followed by space charge-limited current (*SCLC*) at high voltage. The rectification ratio (*RR*) of the device at 71 V is calculated as 3.3. Upon exposure of the sample to dry air for 5 days, diode characteristics are observed with *RR* at 71 V of 100. Shafai and Anthopoulos [37] also investigate the effects of annealing and oxygen doped on the electrical characteristics of the oxygen-doped Au/NiPc/In devices and found that the heat treatment of the sample devices leads to the increase of the contact potential and slight drop in the diode quality factor. Moreover, they investigate the influence of oxygen doping on photovoltaic properties of Au/NiPc/Pb devices. They observed the

photovoltaic effect with power conversion efficiency that less than 1%. Also, they found that the power conversion efficiency of the cell increases dramatically upon exposure to dry air [38].

Menon et al. have been investigated the electrical, optical and structural properties of NiPc thin films and found that annealing alters the activation energy and optical band gap. The first activation energy corresponding to the higher temperature region is associated with the resonant energy involved in a short lived excited state and an intrinsic generation process. The second and third activation energy associated with a short lived charge transfer between impurity and the complex, and is correspond to the impurity conduction. It is shown that as the annealing temperature increases, the intrinsic activation energy increases [39].

Bayrak et al. have studied the electrical properties of peripherally tetra-aldazine substituted novel metal free phthalocyanine and its nickel (*II*) complexes. The conductivity of the nickel films is higher compare to the metal free phthalocyanine. Besides that, the conductivity is increase due to the increase in temperature. This indicates the compounds are semiconductors. The linear relation also shows that the compounds behave as an intrinsic semiconductor in the temperature range of 295–498 K. After 498 K, a small decrease was observed in conductivity of the films. It is well known that, structural/compositional lattice defects increases the localized states and that affects dc conductivity [40].

M.M. El-Nahass et al. have investigated the fabrication and electrical characterization of p-NiPc/n-Si heterojunction by using thin film on n-Si single crystals substrates. The heterojunction shows the diode-like behaviour and exhibits rectifying characteristics with *RR* 4688 at 71 V. The dark *I–V* measurements suggest that the forward current in these junctions involves thermionic emission mechanism at low voltage. In addition, at relative high-applied voltage, a *SCLC* mechanism is operated

with single-trap level, which has a value of 0.57 eV. On the other hand, the reverse current may be reasonably ascribed to a generated current [41].

The NiPc is selected among the phthalocaynine compounds due to its promising characteristics such as high chemical and thermal stability, rather than high charge mobility and reproducibility [37]. However, not many investigations have been conducted on the effects of annealing treatment on the structural, electrical and optical properties of NiPc nanostructures. Neghabi et al. have investigated the structural and optoelectronic properties of annealed NiPc thin films. They found that NiPc thin films annealed at higher temperature exhibit a very smooth surface. Optical analysis indicated that band gap energy of films at different annealing temperatures varied in the range of 3.22–3.28 eV. The measurement of the dark current density–voltage (*J–V*) characteristics of diodes shown that the current density of films annealed at higher temperature for a given bias is greater than the other films annealed at lower temperature [42].

Most of the phthalocyanines compounds have shown a high ideality factor, greater barrier height and large series resistance. The electrical properties of NiPc (without any functional group attached at the periphery) in surface type Schottky diodes have been studied [43] and various electrical parameters of metal/NiPc junctions from current–voltage (*I–V*), capacitance–voltage (*C–V*) and capacitance–frequency (*C–F*) characteristics have been determined. On the other hand, the low mobility, low conductivity and small rectification ratio of these NiPc based diodes have also been observed.

Ahmad et al. have studied the enhancement of electronic and charge transport properties of NiPc by integrating the potassium-tetrasulpho group. They found that the electronic properties of nickel phthalocyanine (NiPc) have been remarkably improved by attaching a potassium-tetrasulpho functional group to form a water soluble derivative

Nickel (*II*) 4,4',4'',4''' potassium tetrasulphophthalocyanine (K_4NiTSPc). The conductivity and mobility of the NiPc derivative based device have been increased by 3–5 orders of magnitude if compared with the NiPc based devices [44]. Sharma et al. has investigated the charge conduction process and photoelectrical properties of Schottky barrier device based on NiTsPc. It is observed that the band gap decreases from 1.7 to 1.56 eV, as the annealing temperature is increased. The decrease in the optical band gap is attributed to the shortening of inter-atomic distance and shifts in the relative positions of the HOMO and LUMO levels due to the temperature dependence of electron lattice interaction. Therefore, the decrease in the band gap increases the width of the orbital. The current value at a given voltage of the device under illumination is higher than that in the dark. This indicates that the absorption of light by the active layer generates carrier contributing photocurrent due to the production of excitons and their subsequent dissociation into the free charge carriers at the Schottky barrier interface [45].

The influence of temperature and frequency on the electrical conductivity and the dielectric properties of NiPc have been studied by Nahass et al. and they found that the *AC* conductivity vary with the angular frequency as the index less than 1 at low temperatures, while at high temperatures the index increased with increasing temperature having a maximum value of 1.37. Such behaviour indicating a hopping conduction mechanism at lower temperatures and a band conduction mechanism dominates at higher temperatures. The *DC* conductivity has also been measured in the considered range of temperature. There is a decrease in the *DC* conductivity in the temperature range from lower to higher temperature, then after that started to increase once again. This behaviour was attributed to drain of oxygen molecules out of the sample during heating [46].

2.2 Template-assisted method

Nanostructured materials can be prepared with the assistance of template membranes of various techniques. One of the techniques is the electrode deposition in which the deposition inside the template pores is determined by two parameters namely reaction rate and diffusion rate. The deposition inside the pores is slower than that the deposition outside the template pores due to the diffusion limitations of reactants inside the pores. The extremely high reaction rate can cause to the closing of the pores at the surface and thus completely stop the diffusion of reactants inside the nanopores. A low temperature of low deposition rate has led to the better morphological of nanostructures, if compared with the nanostructures that grown at high deposition rate [47].

Template-assisted method is a versatile technique to synthesize various forms of nanostructures of desired structure. Nickel nanowires have been successfully synthesised via polycarbonate membrane that acted as a template. The nanowires are grown in multi-porous membranes in cylindrical form of diameter ~90 nm. The diameter and length of nanowires correspond well to those of nanopores in the template. It is suggested that the diameter and length of nanowires can be controlled using different size of nanopores [48]. The nickel nanowires clearly show a significant enhancement in the coercivity properties. This enhancement can be likely attributed to the reduced size of obtained product [49].

Fabrication of nanowire has attracted significant attention due to their important potential applications. Several studies have been performed to produce metal nanowires in templates since the size and the shape of the nanowire can be controlled easily and accurately [50]. Hollow tubular nanostructures have been investigated extensively because of their projected use in drug delivery, catalysis and chemical and biological separation applications [51]. Galvanic displacement reactions, chemical vapour

infiltration, and coating surfaces of colloidal particles [52] have been employed to prepare tubular nanostructures. Electrochemical deposition is a promising technique for the fabrication of nanostructures in a bottom-up trend and it does not require the employment of complex instrumentation [53-55].

Ertan et al. have investigated the fabrications of nickel nanowires and nanotubes by using template-assisted electrochemical deposition process. The results shows that the nickel nanotubes were obtained with 1000 nm pore size polycarbonate membranes without any chemical treatment of pore walls. As the deposition time increases, nanotubes turn into solid rods. As the porosity of the membrane increases, the effective current density decreases due to the larger exposed area. Lower porosity and hence higher current density favours the production of hollow nanostructures as was shown by 1000 nm polycarbonate membranes. They also believe that below a critical pore size, solid rods will be formed through layer by layer mechanism regardless of current density due to the smaller surface area of the pore bottom compared to pore walls. Then they conclude that the morphology of nanostructures is a result of an intricate play between current density, pore size, and aspect ratio [56]. The example to fabricate metallic nanowire by electrochemical deposition into the channels of anodized alumina membrane (AAM) template can be seen in Fig. 6.

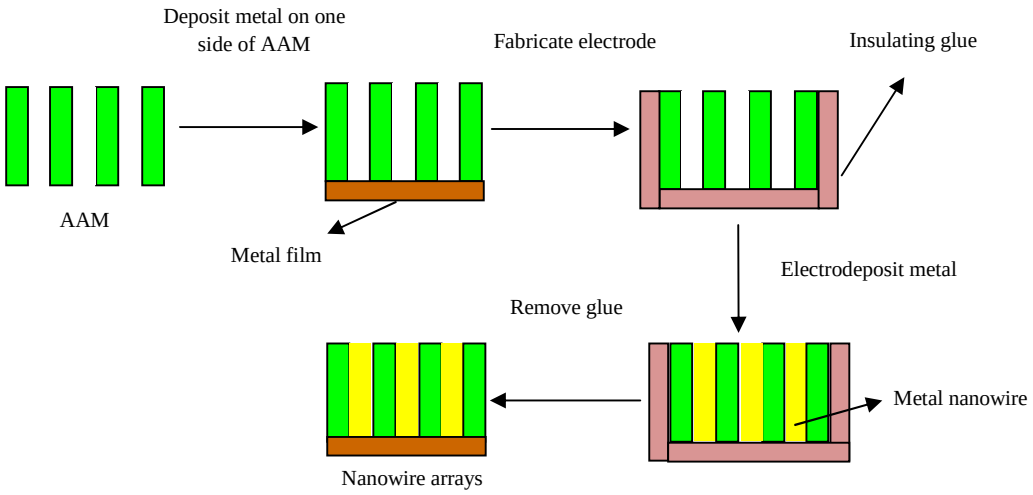

Fig. 6: Schematics of metallic nanowire array fabrication

NiPc nanorods have been obtained on various substrates such as glass, silicon, and indium tin oxide (*ITO*). The nanorods grown on these substrates showed similar morphologies and structures. The device displays a large increase in current upon light illumination, which increases by more than 8 times compared with a dark current. There is a light-induced current output, because a large number of charge carriers can be generated after NiPc nanorods absorb light with photon energy equal to or higher than their band gap energy, which leads to an increase in current [57].

Nanostructure of dioctadecyldimethylammonium bromide (DODAB)/NiTsPc bilayers can be tuned via the layer by layer (*LbL*) technique. The result shows that both DODAB/NiTsPc *LbL* films grow linearly with the number of deposited bilayers, with the higher concentration film presenting higher absorbance values (thicker film), while the lower concentration (thinner film) favours the adsorption of NiTsPc in the monomer form. Optical microscopy and Raman scattering revealed that the thinner *LbL* film is microscopically homogeneous, while the thicker film presents small clusters of NiTsPc on their surface, which is consistent with UV–vis data concerning the equilibrium between monomer/aggregate of NiTsPc in the *LbL* films. Besides, the thinner film presents polydisperse DODAB vesicles on their surface as observed by AFM, while the thicker film presents no vesicle [58]. Silva et al. have studied the morphological properties of NiTsPc multilayer nanostructured film. This approach indicated that the aggregates are rod shaped, which are produced by an adsorption process with two mechanisms which is nucleation in the first stage and diffusion limited growth in another [59]. There is also a research about nickel nanowires can be synthesized via electroless deposition in an organic solvent (ethylene glycol) under a magnetic field. Deposition behaviour of nickel particles and wires were electrochemically investigated at various concentrations of NaOH by an in-situ mixed potential measurement and voltammetry combined with quartz crystal microbalance [60]. The reduction ability of

hydrazine oxidation reactions becomes lower at a lower concentration of NaOH, resulting in a slow deposition rate of nickel and realizing the formation of smooth nickel wires. The rate of nickel deposition reaction can also be controlled by the addition of a complexing agent, $Na_3C_6H_5O_7$. The smooth and high-aspect nickel wires are obtained by adjusting a concentration of $Na_3C_6H_5O7$, and the diameter of nickel wires were controlled from 100 nm to 370 nm by the addition of a nucleating agent, H_2PtCl_6. As a conclusion, the template-directed electrochemical deposition technique has been approved a good alternative approach in synthesizing metallic nanowire arrays and has been widely used in fabricating most metallic nanowire arrays with well-defined structure.

CHAPTER 3: MATERIALS AND METHOD

This section provides a description of the methodology and materials used in this study. The organic materials, NiTsPc were purchased from Sigma Aldrich and used without further purification. The polycarbonate (PC) membrane were purchased from Whatman Corporation and used as template.

3.1 Sample preparation

The PC membranes were cleaned using the ethanol in ultrasonic bath for 10 minutes. A 5 mg/ml and 15 mg/ml of NiTsPc solution were prepared by dissolving 5 mg and 15 mg of NiTsPc powder in 1 ml of deionized water. The polycarbonate membranes were immersed in NiTsPc solution for 1 hour and 24 hours and dried under ambient conditions. The NiTsPc polycarbonate membranes were annealed at different temperatures of 50 °C and 100 °C. Then, stick the upside layer of NiTsPc down to the copper tape. Acetone will be used as solvent in dissolving the PC membrane. The remaining NiTsPc nanostructures will be further cleaned with deionized water. Lastly, the growth of NiTsPc nanostructures can be seen after characterized by field emission scanning electron microscopy (FESEM). The schematic diagram of the preparation steps can be seen in Fig. 7.

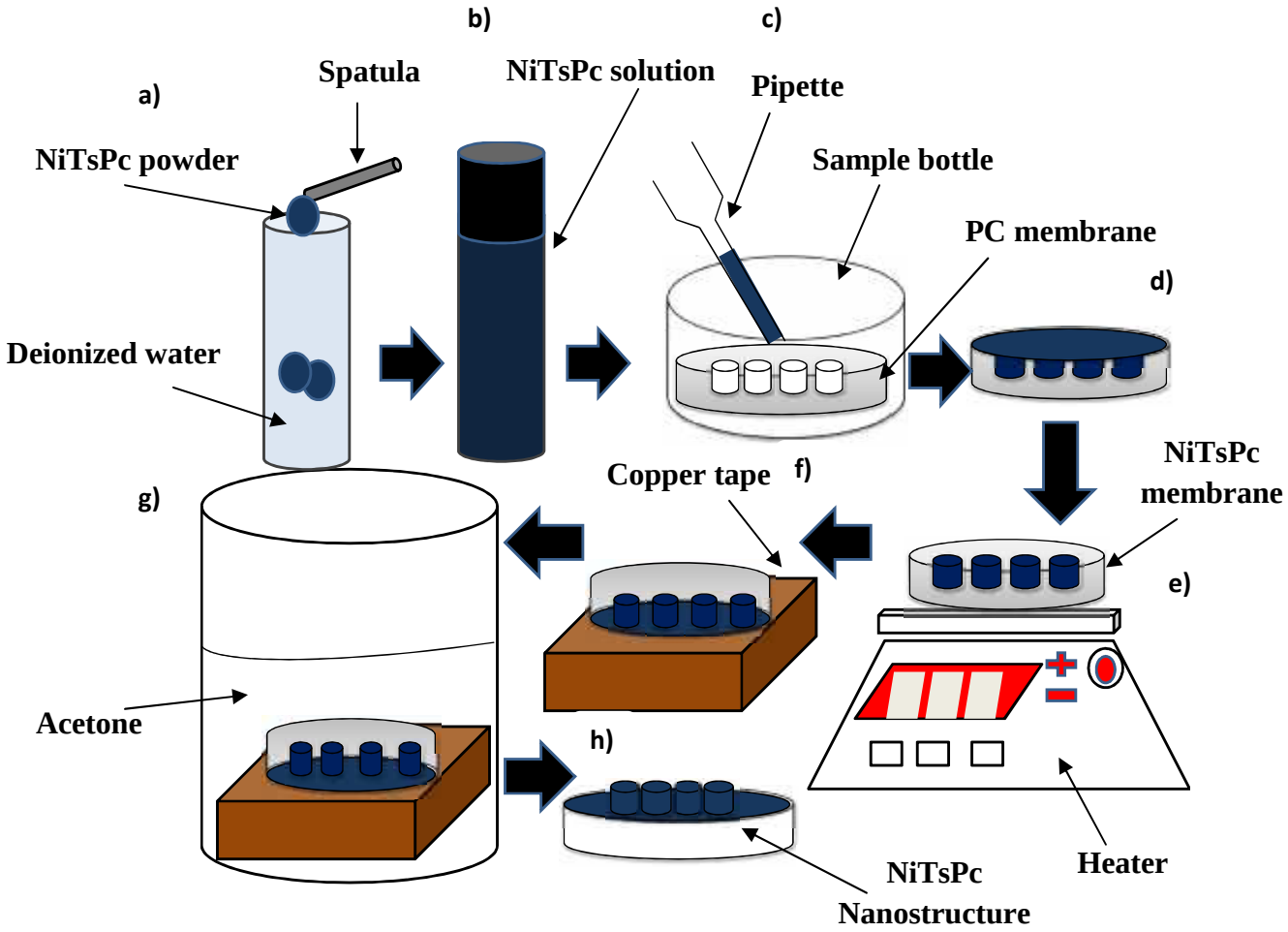

Fig. 7: Schematic diagram of the preparation steps

3.2 Sample characterization

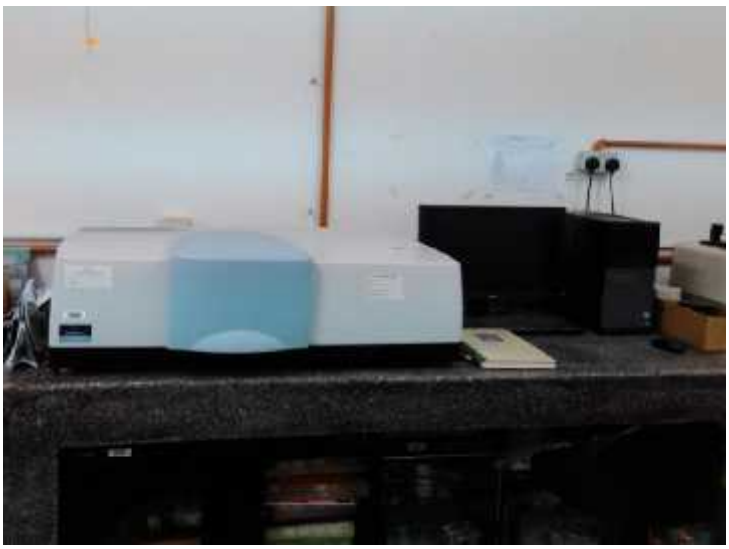

Fig. 8: UV-Vis-NIR spectrometer

We examine the absorption properties of the treated NiTsPc, by using a double beam JASCO V-570 UV – VIS – NIR spectrophotometer. The instrument is shown in Fig. 8. A beam of radiation when strikes to any object it can absorb, transmit, scatter, reflect or it can excite fluorescence. With the scattering process, it can be considered that the radiation is first absorbed and completely re-emitted uniformly in all directions. With the fluorescence, a photon is first absorbed and excites the molecule to a higher energy state, but the molecule then drops back to an intermediate energy level by re-emitting a photon. Since some of the energy of the incident photon is retained in the molecule which is lost by a non-radiative process such as collision with another molecule or the emitted photon has less energy and hence a longer wavelength than the absorbed photon. Similar to the scattering, fluorescent radiation is also emitted uniformly in all directions.

The processes concerned in UV-Vis-NIR absorption spectrometry are absorption and transmission. Usually the conditions under which the sample is examined are chosen to keep reflection, scatter and fluorescence to a minimum. In the ultraviolet and visible regions of the electromagnetic spectrum, the bands observed are usually not specific enough to allow a positive identification of an unknown sample, although this data may be used to confirm its nature deduced from its infrared spectrum or by other techniques. Ultraviolet and visible spectrometry is almost entirely used for quantitative analysis; that is, the estimation of the amount of a compound known to be present in the sample.

Fig. 9: Renishaw Micro-Raman

We examine the information about the phase of molecules using via Renishaw Micro-Raman as shown in Fig. 9. Raman spectroscopy comprises the family of spectral measurements made on molecular media based on inelastic scattering of monochromatic radiation. When a sample is irradiated with an intense monochromatic light source usually a laser, most of the radiation is scattered by the sample at the same wavelength as the incoming laser (Rayleigh scattering). A small proportion of the incoming light approximately one photon out of a million is scattered at a wavelength that is shifted from the original laser wavelength (Raman scattering). During this process energy is exchanged between the photon and the molecule such that the scattered photon is of higher or lower energy than the incident photon. The difference in energy is made up by a change in the rotational and vibrational energy of the molecule and gives information on its energy levels.

In dispersive Raman, it is accomplished by focusing the Raman scattered light onto a diffraction grating, which splits the beam into its constituent wavelengths. These are directed onto a charge-coupled device (CCD) detector. Typical laser wavelengths are 780 nm, 633 nm, 532 nm, and 473 nm; others are also used. Spectral resolution

determines the amount of detail that can be seen in the spectrum. Spectral resolution is determined by the diffraction grating dispersion and by the optical design of the spectrograph. Gratings have many lines into the surface, which disperse the incoming light. The higher the number of grating lines per unit length, the broader the dispersion angle and the higher the spectral resolution obtained. To achieve higher resolution, it is necessary to move either the grating or the detector to collect sequential segments of the spectrum.

Fig. 10: Renishaw Micro-Raman (PL)

Photoluminescence (PL) is used to do a compositional analysis of the epitaxial layer of compound and evaluation of surfaces of a sample. PL incorporated with Raman attachment as shown in Fig. 10. Photoluminescence spectroscopy is a non-contact, non-destructive method of probing the electronic structure of materials. In essence, light is directed onto a sample, where it is absorbed and where a process called photo-excitation can occur. The photo-excitation causes the electrons (valence band) of the material to jump to a higher electronic state (excitation band), and will then release energy,

(photons) as it relaxes and returns to back to a lower energy level. The emission of light or luminescence through this process is photoluminescence.

Current and voltage (*I-V*) characteristic of the NiTsPc were recorded by Jandel Universal probe station in a clean and shielded box at room temperature as shown in Fig. 11. Four point probe characterization is a standard method for studying the electrical properties of solids and thin films. The probe spacing in four-point probe technique has to be reduced to micro-scale to obtain expected surface sensitivity and spatial resolution. Therefore, microscopic four-point probes (M4PPs) need to be combined with some microscopy techniques. Two types of M4PPs systems have been developed in the past few years, which are monolithic micro-four-point probe and four-point scanning tunnelling microscopy probe approaches.

Fig. 11: Jandel Universal probe station

A current is made to flow through the outer probe pair and a voltage drop is measured across the inner pair using a voltmeter with ultrahigh impedance. As a result, the measured voltage drop *'V'* is predominantly occurred across the semiconductor surface due to the current *'I'* flowing through the sample. The four point-probe

resistance *'R'* is then given by $R=\frac{V}{I}$. For a measurement of semiconductor crystal or thin films, the M4PPs current will in principle flow through three channels, which is the surface state, surface space-charge layer and bulk state. It is thus very difficult to precisely characterize the electrical properties owing to current contributions from these entangled channels. If the probe spacing is less than the thickness of the space-charge layer, the as-measured current will be mainly resulted from the surface region, which can thus diminish the bulk contribution. Reducing the probe spacing, we can minimize the influences of leakage current and surface defects and thus maximize the surface sensitivity.

A basic property of a conductive material is its electrical resistivity. The electrical resistivity is determined by the availability of "free electrons" in the material. In turn the availability of free electrons is determined by the physical binding properties of the material on a molecular level. Other important properties of the material are related to the physical binding properties and therefore to the electrical resistivity of the material. Much may be learned about the properties of a material by measuring its resistivity. An important example is the characterization of semiconductor materials where the resistivity is strongly related to the level of purposely added impurities. Measurement of the resistivity is used to both characterize the material and as a process control parameter for the semiconductor manufacturing process. Resistivity measurements are also used to characterize many other materials. For low resistivity, the best method is the four point probing. Current is sent in two probes and voltage is

measured by two other probes. So, the measured voltage is really that circulate into the sample with no current. So there is no potential difference into the wires and contact and spreading resistance are not high. Measure will be more accurate.

Fig. 12: Field emission scanning electron microscopy

The morphological properties of the NiTsPc are characterized using JSM 7600-F, JEOL L.td, Tokyo, Japan as shown in Fig. 12. Field emission scanning electron microscope (FESEM) mainly use to scan a sample surface with a finely converged electron beam in a vacuum, detects the information (signals) produced at that time from the sample, and presents an enlarged image of the sample surface on the monitor screen. By irradiating the sample with an electron beam in a vacuum, secondary electrons, backscattered electrons, characteristic x-rays and other signals are generated. The FESEM mainly uses the secondary electron or backscattered electron signals to form an image. Secondary electrons are produced near the surface, and the image obtained upon detecting these electrons reflects the fine topographical structure of the sample. Backscattered electrons are those reflected upon striking the atoms composing the sample, and the number of these electrons is dependent on the composition of the sample. A backscattered image therefore reflects the compositional distribution on the

sample surface. Besides, an x-ray detector can be mounted to the FESEM for conducting elemental analysis. They are several components in FESEM such electron gun, condenser lens, deflection coils, objective lens, secondary electron detector, display and vacuum pump. Each component has its own function.

CHAPTER 4: RESULTS AND DISCUSSION

4.1: Optical properties

The absorption spectra of NiTsPc nanostructures that annealed at 50 °C and 100 °C of different concentration (5 mg/ml and 15 mg/ml) and different immersion time (1 hour and 24 hour) are shown in Fig. 13 (a) and Fig. 13 (b), respectively. NiTsPc nanostructures have exhibited two predominant peaks that assigned as *B* and *Q* bands. At the *Q* band, the peak absorption at 630 nm is corresponded to the first π–π^* transition on the phthalocyanine macrocyle. In addition, a shoulder peak at around 670 nm is assigned to the second π–π^* transition.

At the *B* band, a strong absorption peak at 290 nm and a shoulder peak around 356 nm indicate the presence of a d-band associated with the central atom which is nickel [61]. This attributes to *π–d* and partially occupied d-π^* transitions [7]. It can be observed that a small red-shift of *Q* band has been recorded from the absorption spectra of NiTsPc nanostructures of 15 mg/ml and 24 hours immersion time of both annealing times. The red-shift is correlated with the higher absorption intensity obtained by these NiTsPc nanostructures. Absorption intensity of NiTsPc nanostructures (15 mg/ml and 24 hours) annealed at 100 °C is higher than that annealed at 50 °C. In addition, there is a peak broadening at *Q* and *B* bands of NiTsPc nanostructures annealed at higher temperature.

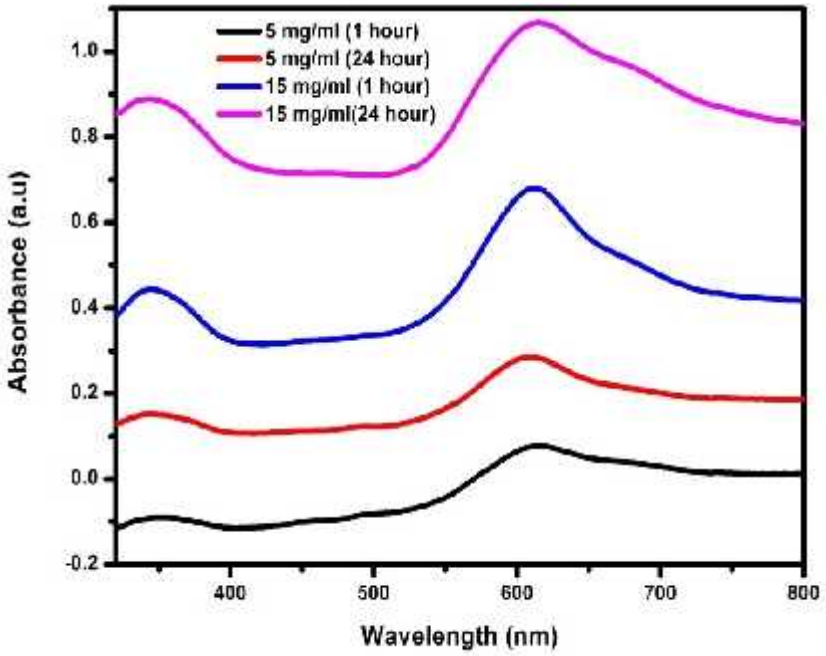

Fig. 13 (a): Absorption spectra of NiTsPc nanostructures at 50 °C

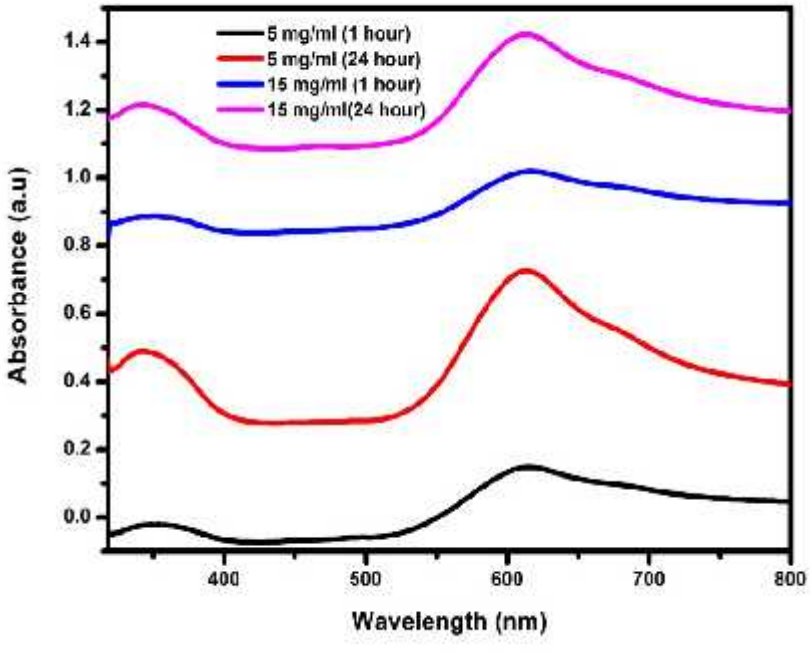

Fig. 13 (b): Absorption spectra of NiTsPc nanostructures at 100 °C

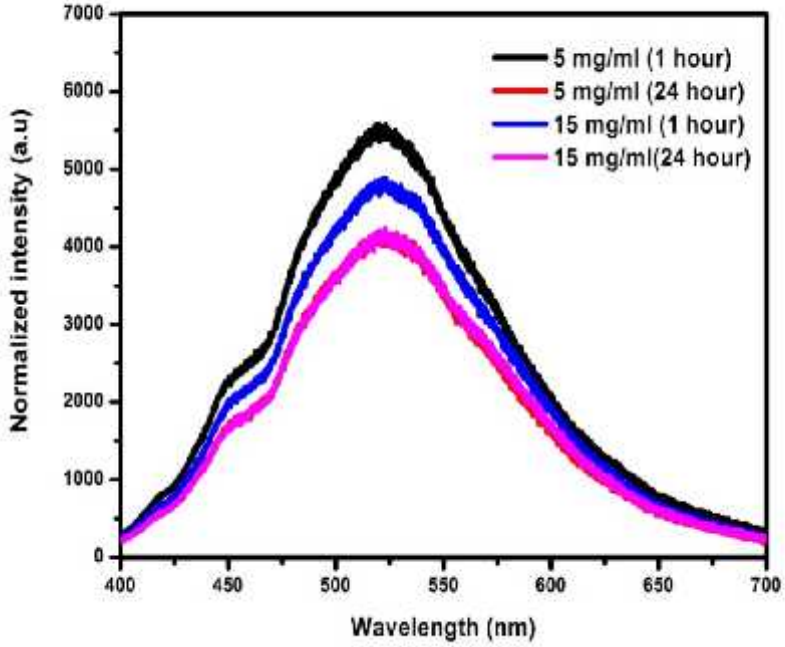

Fig. 14 (a): Photoluminescence spectra of NiTsPc nanostructures at 50 °C

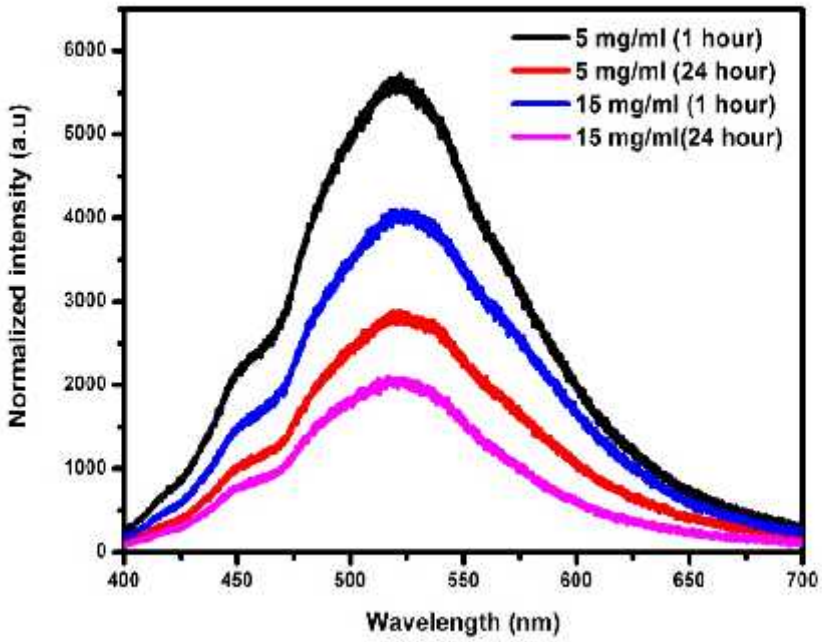

Fig. 14 (b): Photoluminescence spectra of NiTsPc nanostructures at 100 °C

The charge transfer behaviour of NiTsPc nanostructures can be examined from the photoluminescence spectra shown in Fig. 14 (a) and Fig. 14 (b). The photoluminescence (PL) intensity of NiTsPc nanostructures is quenched to some extent as the solution concentration of NiTsPc is increased to 15 mg/ml and immersed for 24 hour of both annealing temperatures (50 °C and 100°C). The PL quenching represents the efficient charge transfer at the donor/acceptor interface [62]. A better charge transfer is obtained from the NiTsPc nanostructures that synthesised from the higher solution concentration and longer immersion time. A better percolation path for the charge carrier to be transported within the system could be achieved from the changes in morphological properties of increased surface areas and interfaces.

Fundamentally, the chemical molecular structure of NiTsPc is defined as a planar molecule consisting of 57 atoms. Therefore, the characterizations of the vibration follow the square planar molecule. Fig. 15 (a) and Fig. 15 (b) show the Raman spectra of NiTsPc nanostructures grown from 50 °C and 100 °C, respectively, with no shift at the band position is observed. There are two protruding peaks appear around 1355 and 1585 cm $^{-1}$, and assigned as *D* and *G* band, respectively. The *D* band indicates the presence of six fold aromatic ring in NiTsPc nanostructures. On the other hand, the *G* band indicates the presence of a six fold aromatic ring and chain [63]. A tentative band assignment of vibration of each Raman active mode is tabulated in Table 1. It can be found that the *G* peak is triggered from the vibration of C-N and C-N=C-C=C. The latter vibration shows that the sixfold aromatic ring has been distorted and then initiates the opening of the sixfold aromatic ring from the chemical structure of NiTsPc [64].

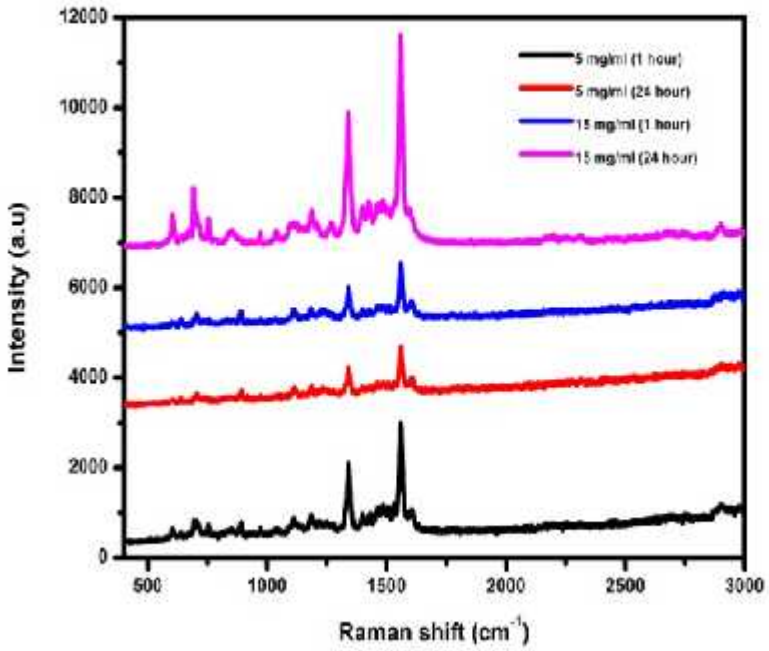

Fig. 15 (a): Raman spectra of NiTsPc nanostructures at 50 °C

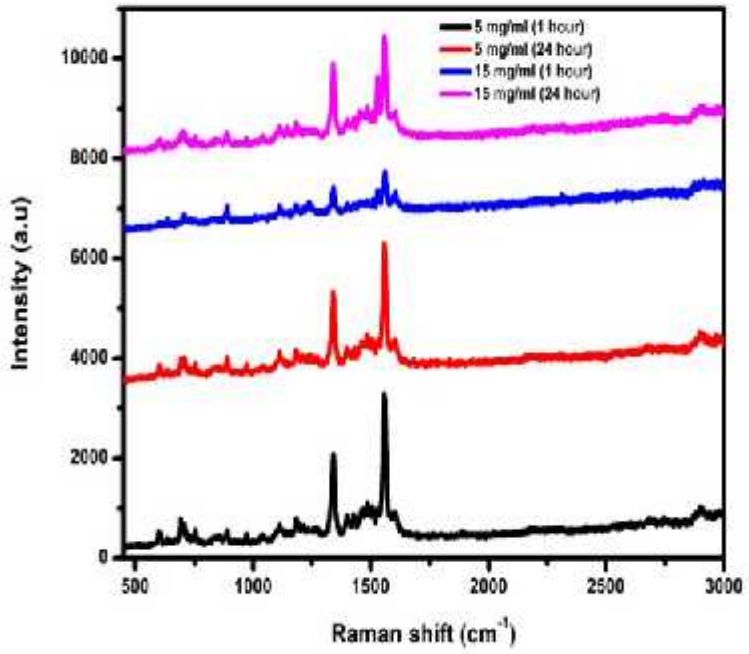

Fig. 15 (b): Raman spectra of NiTsPc nanostructures at 100 °C

Band Position (cm^{-1})	Band assignment
604 – 690	C-N, Ni-N, C=N
1035 – 1094	C-N, C=N, C=C-C
1181 - 1339	C=C-C
1550 - 1558	C-N, C-N=C-C=C

Table 1: Tentative band assignment of NiTsPc nanostructures

4.2: Morphological properties

Field emission scanning electron microscopy (FESEM) is used to study the morphological changes of NiTsPc nanostructures annealed at different temperatures, synthesised at different solution concentrationand immersion time. Fig. 16 (a) – Fig. 16 (i) present the FESEM images of polycarbonate membrane and NiTsPc nanostructures of different synthesised parameters. Polycarbonate membrane has a nominal pore diameter of ~ 50 nm and membrane diameter of ~ 25 mm. As shown in Fig. 16 (b) to Fig. 16 (i), the surface morphology of NiTsPc nanostructures varies substantially with the annealing temperature, solution concentration and immersion time. As the annealing temperature increases, the NiTsPc nanostructures become denser and the diameter become smaller. The surface topography of NiTsPc nanostructures has improved and the nanostructure network becomes more continuous. The nucleation and growth process of nanostructures on the polycarbonate membrane has been altered with the assistance of increased annealing temperature [65].

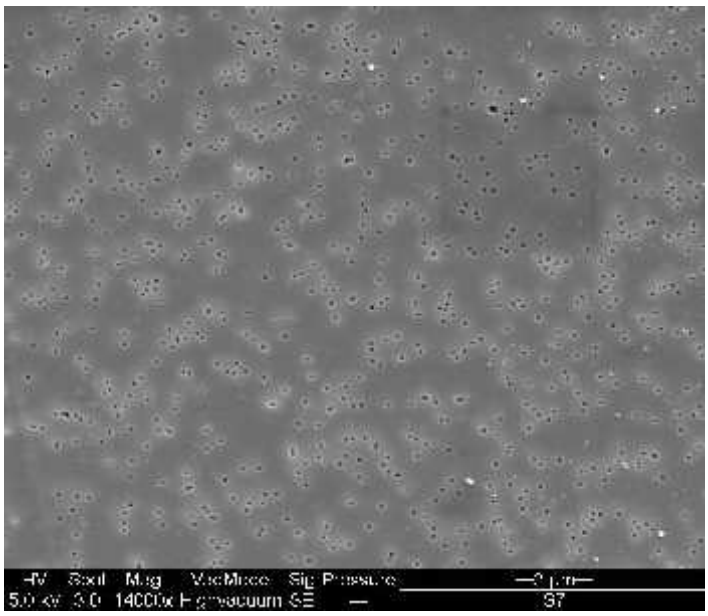

Fig. 16 (a): FESEM image of polycarbonate membrane

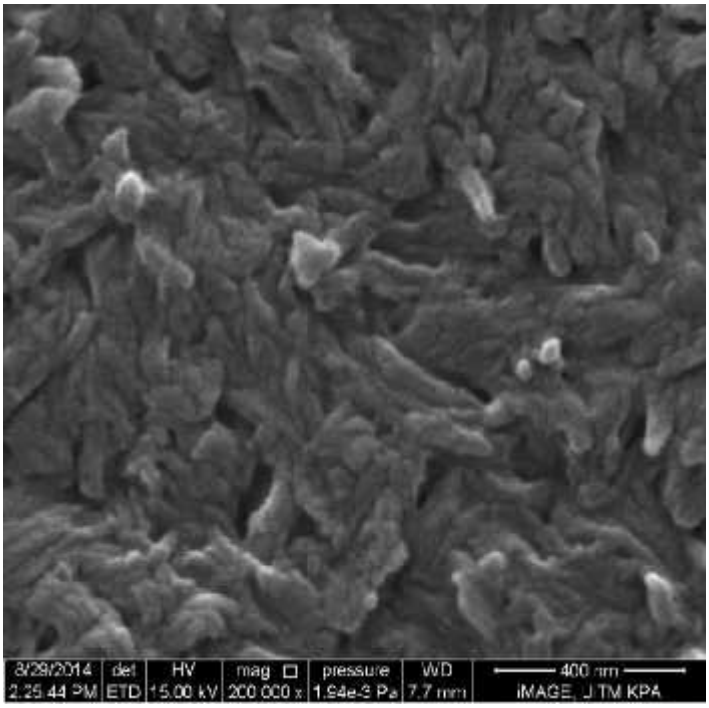

Fig. 16 (b): FESEM image of NiTsPc nanostructures at 50 °C (5 mg/ml-1 hour)

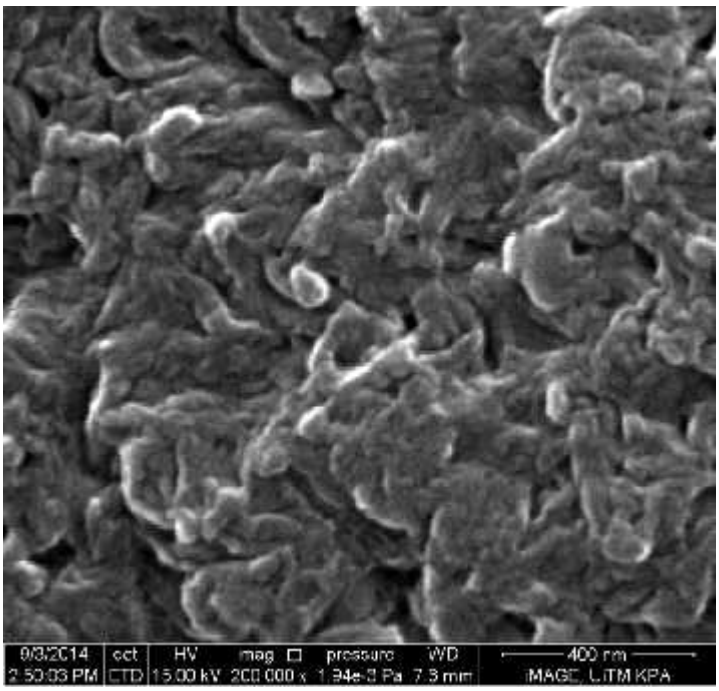

Fig. 16 (c): FESEM image of NiTsPc nanostructures at 50 °C (5 mg/ml-24 hour)

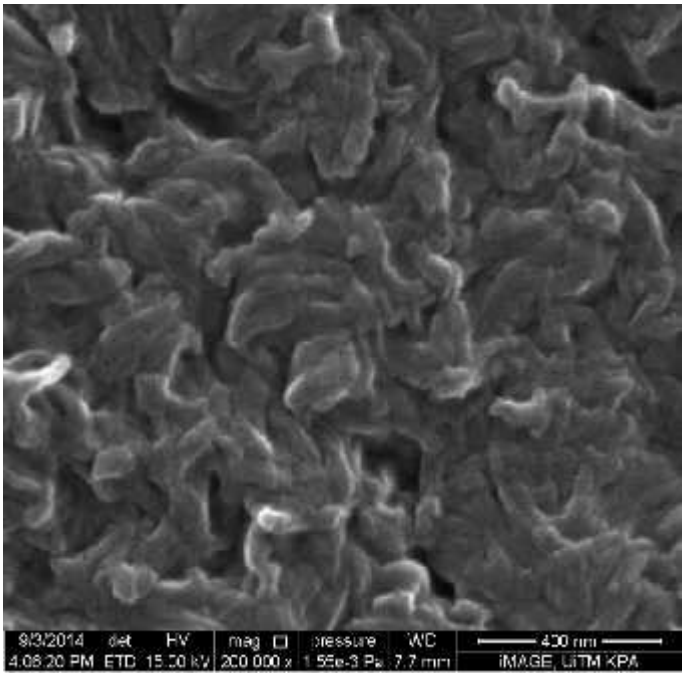

Fig. 16 (d): FESEM image of NiTsPc nanostructures at 50 °C (15 mg/ml-1 hour)

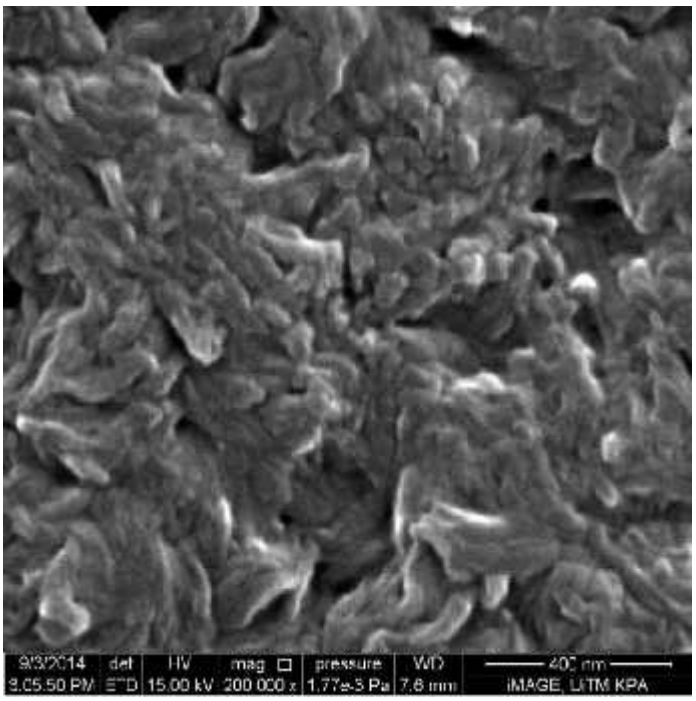

Fig. 16 (e): FESEM image of NiTsPc nanostructures at 50 °C (15 mg/ml-24 hour)

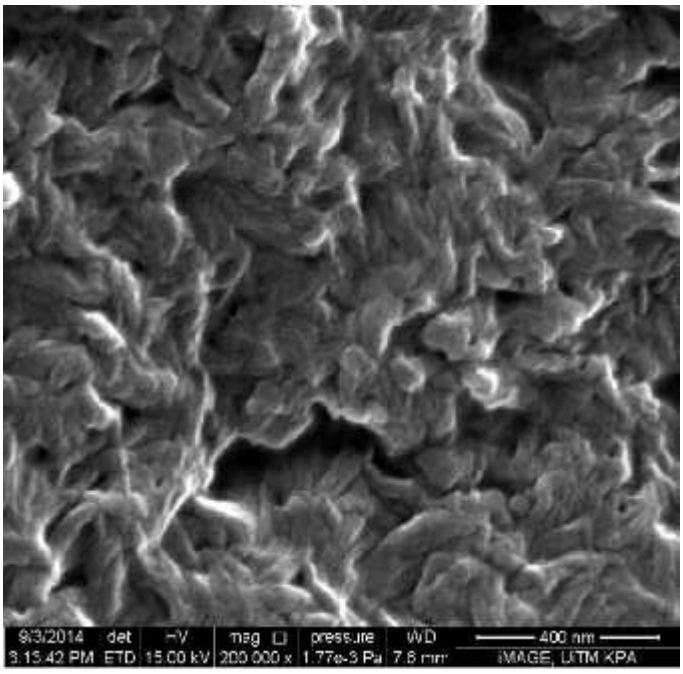

Fig. 16 (f): FESEM image of NiTsPc nanostructures at 100 °C (5 mg/ml-1 hour)

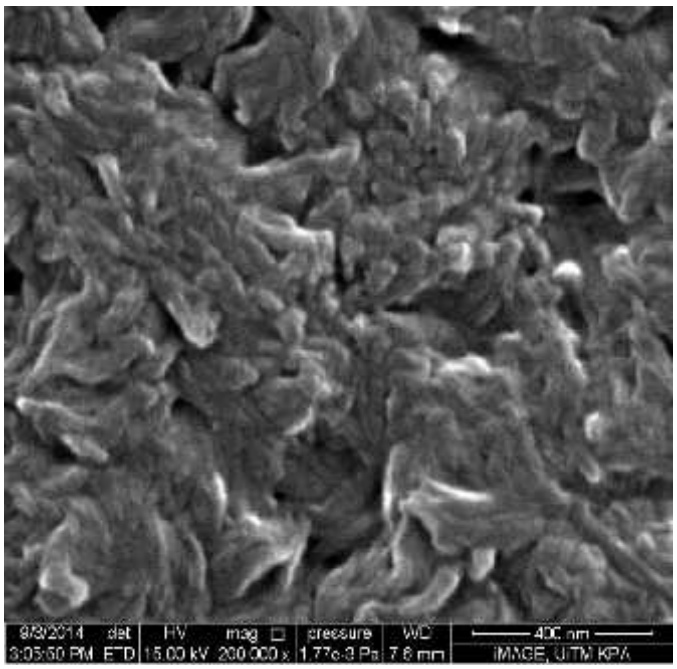

Fig. 16 (g): FESEM image of NiTsPc nanostructures at 100 °C (5 mg/ml-24 hour)

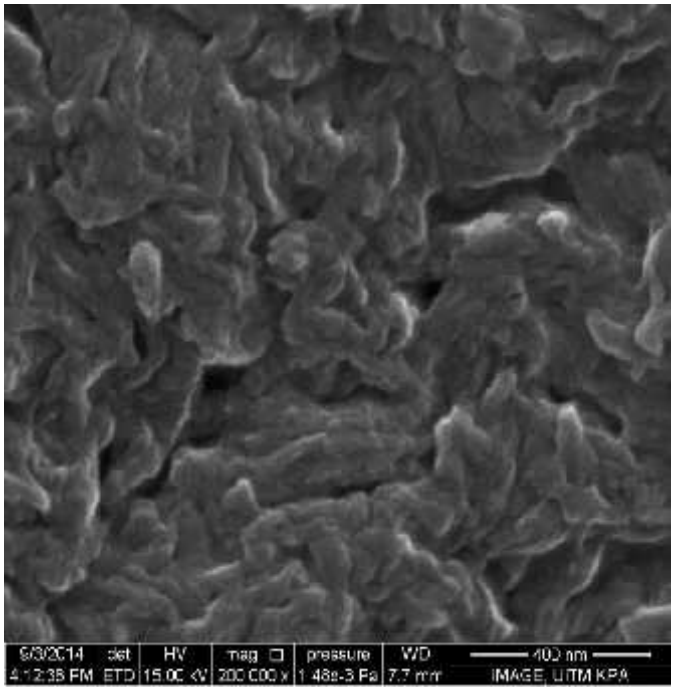

Fig. 16 (h): FESEM image of NiTsPc nanostructures at 100 °C (15 mg/ml-1 hour)

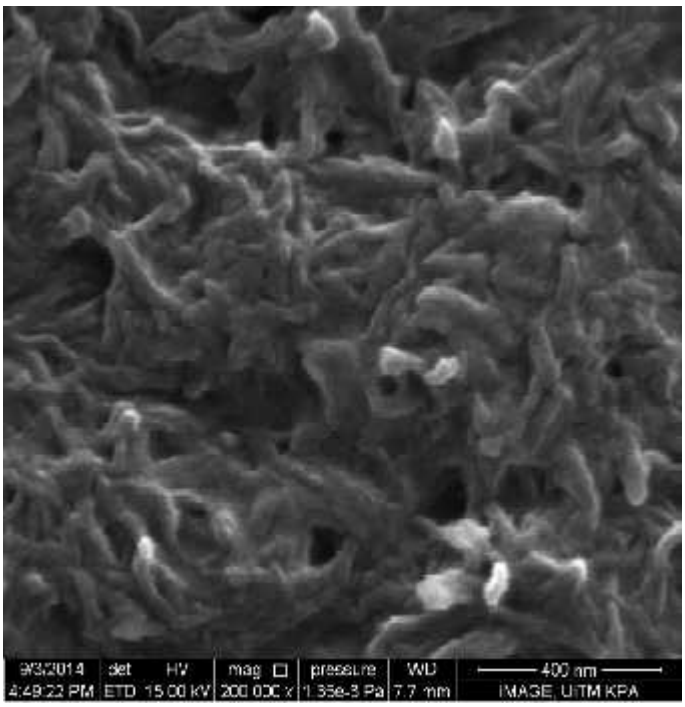

Fig. 16 (i): FESEM image of NiTsPc nanostructures at 100 °C (15 mg/ml-24 hour)

The presence of defects, such as subparticles and pinholes at phthalocyanine and other layer interface could decrease the charge carrier transport. To ensure the higher efficiency of charge carrier transport within the NiTsPc nanostructures system, the surface areas and interfaces within the system have to be increased. Optical properties and morphological properties of NiTsPc nanostructures have a correlation in determining the generation, dissociation and recombination of charge carriers. Fundamentally, excitons (electrons and holes) are generated prior to the dissociation process which normally occurred at the interfaces. Thin films structure has a limitation of interfaces if compared with the nanostructures which in this study, the fibrous-like nanostructures are observed. The formation of NiTsPc nanostructures has improved the properties of the existing NiTsPc thin films.

4.3 Electrical properties

The analysis of *I-V* measurement is extremely useful for the identification of the transport mechanism that controlled the conduction process of devices. Fig. 17 (a) and Fig. 17 (b) show the *I-V* characteristic of NiTsPc nanostructures that annealed at 50°C and 100 °C, respectively. The figure demonstrates the dependences of the current on the voltage. It can be seen that the increasing of the current at a given voltage is not much. It shows an exponential increase in the current with the applied voltage at the junction. This exponential dependence can be attributed to the formation of depletion region. Obviously, the surface morphological properties of phthalocyanine can affect the electrical characteristics and performance of the electronic devices [66].

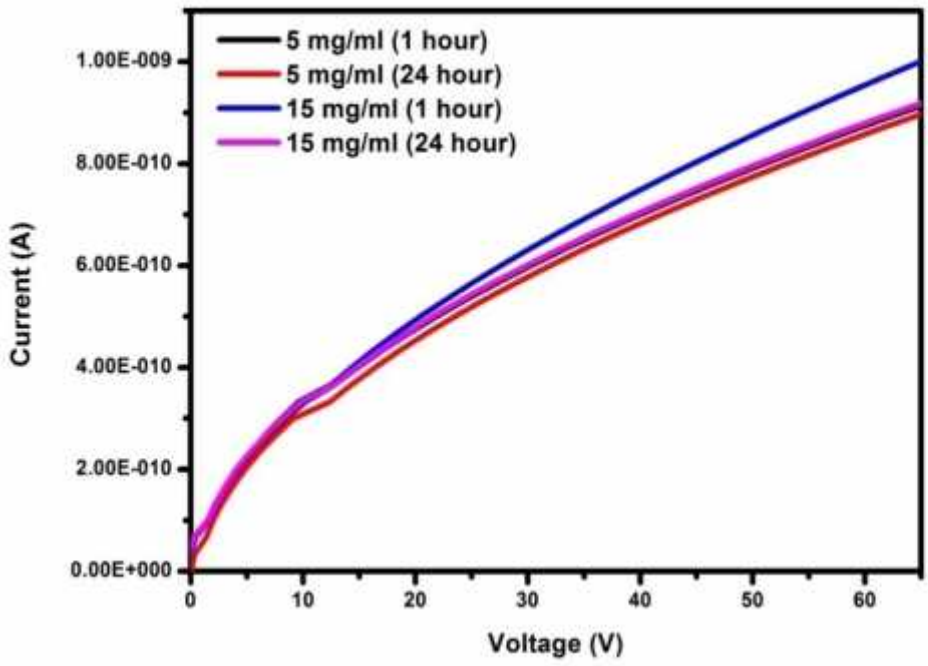

Fig. 17 (a): *I-V* characteristic of NiTsPc nanostructures at 50 °C

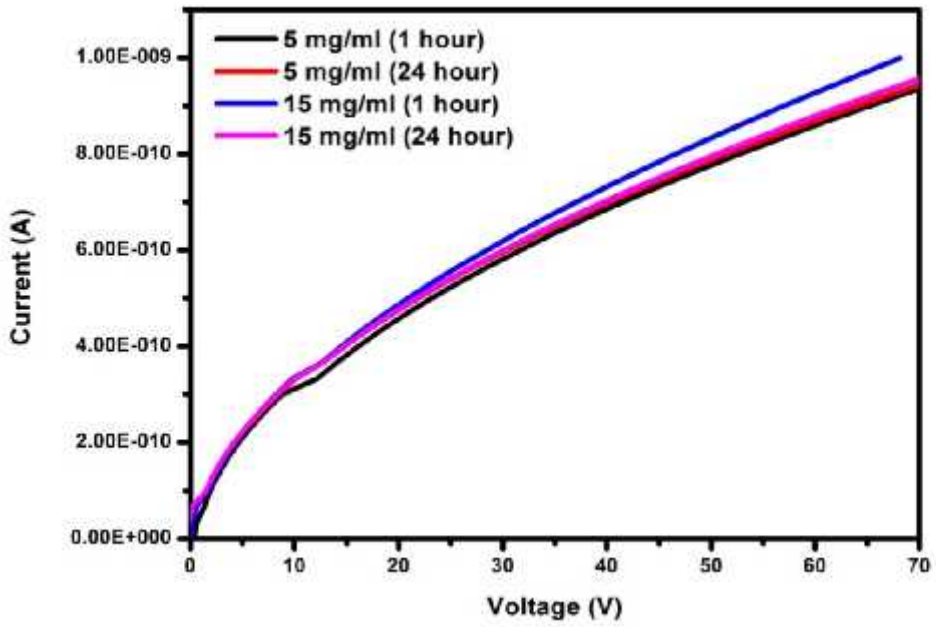

Fig. 17 (b): *I-V* characteristic of NiTsPc nanostructures at 100 °C

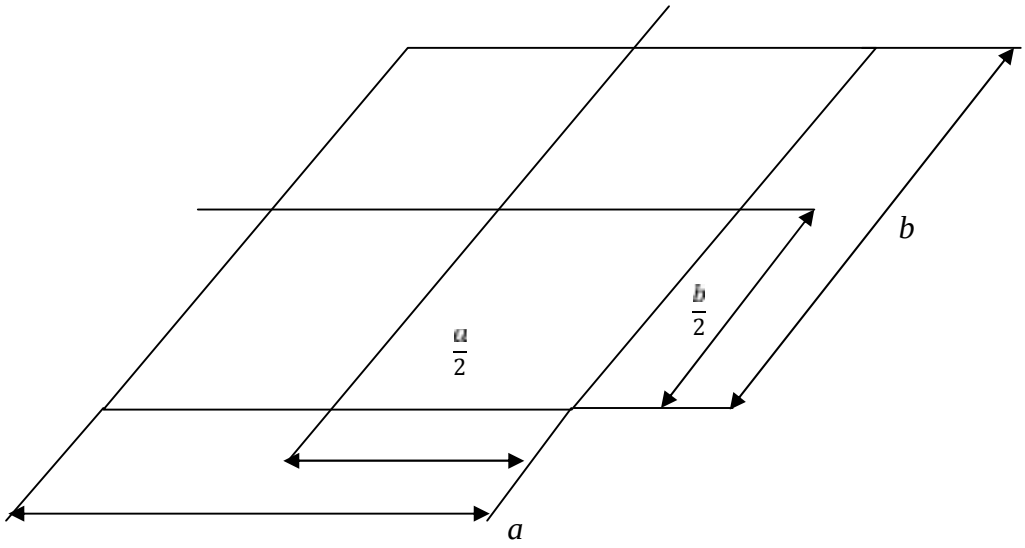

Fig. 18: Schematic diagram of the rectangular sample

The conductivity of the NiTsPc nanostructures can be calculated using Haldor Topsoe technique. The configuration of the rectangular slice that have a thickness, $t < \frac{s}{2}$ can be seen in Fig. 18. The value of s is 2.0 mm, and a and b is 7.0 mm, respectively. The geometry of sample determines the correction factors that need to be applied, and also the position of the probes on the sample and the spacing between the probes. The need for correction factors is due to the proximity of a boundary which limits the possible current paths in the sample.

The resistivity is given by:

$$\rho = G\frac{V}{I} \quad , \qquad G = \frac{\pi}{\ln 2} \cdot t \cdot R_1\left(\frac{b}{s}, \frac{a}{b}\right)$$

where $\frac{\pi}{\ln 2} \cdot t = 4.5324 \cdot t$, is the geometric factor for an infinitely large slice of thickness $t << s$ and $R_1\left(\frac{b}{s}, \frac{a}{b}\right)$ is the additional correction to apply because of the finite, rectangular shape. The information on the thickness, geometric factor, ratio of $\frac{V}{I}$, resistivity and conductivity of each sample at 50 °C and 100 °C can be seen in Table 2 and Table 3, respectively.

The conductivity of NiTsPc nanostructures is decrease at the higher annealing temperature. However, the decrease between two different annealing temperatures has no significant differences. The thicker sample tends to have a lower conductivity which may be due to the high resistance.

Concentration/ annealing time	Thickness, t (μm)	Geometric factor, G ($\times 10^{-6}$)	$R = \frac{V}{I}$ ($\times 10^{9}$) Ω	Resistivity, ρ ($\times 10^{6}$) Ω cm	Conductivity, σ ($\times 10^{-8}$) S/cm
5 mg/ml (1 hour)	10.32	32.1	0.8	2.57	0.389
5 mg/ml (24 hour)	10.43	32.5	0.8	2.60	0.385
15 mg/ml (1 hour)	10.56	32.8	0.8	2.62	0.381
15 mg/ml (24 hour)	10.81	33.7	0.8	2.70	0.371

Table 2: The conductivity of the NiTsPc nanostuctures at 50 °C

Concentration/ annealing time	Thickness, t (μm)	Geometric factor, G ($\times 10^{-6}$)	$R = \frac{V}{I}$ ($\times 10^{9}$) Ω	Resistivity, ρ ($\times 10^{6}$) Ω cm	Conductivity, σ ($\times 10^{-8}$) S/cm
5 mg/ml (1 hour)	10.79	33.6	0.8	2.69	0.372
5 mg/ml (24 hour)	10.86	33.8	0.8	2.70	0.369
15 mg/ml (1 hour)	10.90	33.9	0.8	2.71	0.368
15 mg/ml (24 hour)	10.95	34.1	0.8	2.73	0.367

Table 3: The conductivity of the NiTsPc nanostuctures at 100 °C

CHAPTER 5: SUMMARY AND CONCLUSION

Nickel tetrasulphonatedphthlocyanine (NiTsPc) nanostructures were successfully synthesised via polycarbonate membrane of immersion technique. NiTsPc nanostructures were characterised by UV-Vis spectroscopy, photoluminescence (PL) spectroscopy, Raman spectroscopy, field emission scanning electron microscopy (FESEM) and four point probes. The UV-vis absorption intensity of NiTsPc nanostructures annealed at 100°C is higher than that at 50°C. NiTsPc nanostructures have exhibited two absorption peaks that assigned as *B* and *Q* bands. The *Q* band at 630 nm is corresponded to the first π–π^* transition on the phthalocyanine macrocyle. Meanwhile, a shoulder peak at 670 nm is attributed to the second π–π^* transition. PL quenching of NiTsPc nanostructures represents an efficient charge transfer at the interfaces. A better charge transfer is obtained at the interfaces of nanostructures that annealed at the higher temperature of longer immersion time. The structural properties of NiTsPc nanostructures are preserved although different synthesis parameters were implemented, which proven from the observation with no shift at the Raman bands. There are two protruding peaks at 1355 and 1585 cm^{-1} in the Raman spectra, which assigned as *D* and *G* band, respectively. The surface morphology and topography of NiTsPc nanostructures of 15 mg/ml that annealed at 100°C and immersed for 24 hour, has improved and enhanced. The network structure becomes more continuous and smaller fibrous diameter is obtained. The conductivity of NiTsPc nanostructures is decrease at the higher annealing temperature. However, the decrease between two different annealing temperatures has no significant differences. The thicker sample tends to have a lower conductivity which may be due to the high resistance. The use of polycarbonate membrane as the template can be the alternative way to produce nanostructures. The results also show that NiTsPc nanostructures that synthesized via

polycarbonate membrane can be considered as a new material in photovoltaic applications.

REFERENCES

1. De la Torre, G., C.G. Claessens, and T. Torres, *Phthalocyanines: old dyes, new materials. Putting color in nanotechnology.* Chemical Communications, 2007(20): p. 2000-2015.
2. Salan, Ü., et al., *Photovoltaic and electrocatalytic properties of novel ball-type phthalocyanines bridged with four dicumarol.* Dalton Transactions, 2012. **41**(17): p. 5177-5187.
3. Bezzu, C.G., et al., *Synthesis and crystal structure of a novel phthalocyanine-calixarene conjugate.* Journal of Porphyrins and Phthalocyanines, 2011. **15**(07n08): p. 686-690.
4. Nyokong, T., *Effects of substituents on the photochemical and photophysical properties of main group metal phthalocyanines.* Coordination Chemistry Reviews, 2007. **251**(13): p. 1707-1722.
5. Ponce, I., et al., *Enhanced catalytic activity of Fe phthalocyanines linked to Au (111) via conjugated self-assembled monolayers of aromatic thiols for O reduction.* Electrochemistry Communications, 2011. **13**(11): p. 1182-1185.
6. Seoudi, R., G. El-Bahy, and Z. El Sayed, *FTIR, TGA and DC electrical conductivity studies of phthalocyanine and its complexes.* Journal of molecular structure, 2005. **753**(1): p. 119-126.
7. El-Nahass, M., et al., *Dispersion studies and electronic transitions in nickel phthalocyanine thin films.* Optics & Laser Technology, 2005. **37**(7): p. 513-523.
8. Del Cano, T., et al., *Characterization of evaporated trivalent and tetravalent phthalocyanines thin films: different degree of organization.* Applied surface science, 2005. **246**(4): p. 327-333.
9. He, T., et al., *Applied Magnetism, Magnetic Materials And Superconductivity.* Journal of physics: Applied physics, 2004. **37**(22-24): p. 3453.

10. Ragoussi, M.E., et al., *Carboxyethynyl Anchoring Ligands: A Means to Improving the Efficiency of Phthalocyanine-Sensitized Solar Cells.* Angewandte Chemie International Edition, 2012. **51**(18): p. 4375-4378.

11. Schlettwein, D., H. Tada, and S. Mashiko, *Organic molecular beam epitaxial growth of substituted phthalocyanine thin films–tetrapyridotetraazaporhyrins on alkali halide (100) surfaces.* Thin Solid Films, 1998. **331**(1): p. 117-130.

12. Tsankov, D., et al., *Infrared ellipsometry of Langmuir-Blodgett films on gold. Toward interpreting the molecular orientation.* Langmuir, 2002. **18**(17): p. 6559-6564.

13. Sharma, G., V. Singh Choudhary, and M. Roy, *Effect of annealing on the optical, electrical, and photovoltaic properties of bulk hetero-junction device based on PPAT: TY blend.* Solar energy materials and solar cells, 2007. **91**(4): p. 275-284.

14. Milián-Medina, B. and I. Nanoscience, *Fluoro-Functionalization of Vinylene Units in a Polyarylenevinylene for Polymer Solar Cells: Impact of Fluorination on Morphological and Optical Properties and on Photovoltaic Performances.*

15. Gebeyehu, D., et al., *Bulk-heterojunction photovoltaic devices based on donor–acceptor organic small molecule blends.* Solar energy materials and solar cells, 2003. **79**(1): p. 81-92.

16. Osasa, T., et al., *Photocarrier generation in organic thin-film solar cells with an organic heterojunction.* Solar energy materials and solar cells, 2006. **90**(10): p. 1519-1526.

17. Sharma, G., V.S. Choudhary, and M. Roy, *Electrical and photovoltaic properties of devices based on PbPc–TiO thin films.* Solar energy materials and solar cells, 2007. **91**(12): p. 1087-1096.

18. Lane, P., et al., *Electroabsorption studies of phthalocyanine/perylene solar cells.* Solar energy materials and solar cells, 2000. **63**(1): p. 3-13.

19. Singh, V., et al., *Copper-phthalocyanine-based organic solar cells with high open-circuit voltage.* Applied Physics Letters, 2005. **86**(8): p. 082106-082106-3.

20. Terao, Y., H. Sasabe, and C. Adachi, *Correlation of hole mobility, exciton diffusion length, and solar cell characteristics in phthalocyanine/fullerene organic solar cells.* Applied Physics Letters, 2007. **90**(10): p. 103515-103515-3.

21. Parra, V., et al., *On the effect of ammonia and wet atmospheres on the conducting properties of different lutetium bisphthalocyanine thin films.* Thin Solid Films, 2008. **516**(24): p. 9012-9019.

22. Bouvet, M., *Phthalocyanine-based field-effect transistors as gas sensors.* Analytical and bioanalytical chemistry, 2006. **384**(2): p. 366-373.

23. Yang, F. and S.R. Forrest, *Photocurrent generation in nanostructured organic solar cells.* ACS nano, 2008. **2**(5): p. 1022-1032.

24. Bilgin, A., B. Ertem, and Y. Gök, *Synthesis and characterization of new metal-free and metallophthalocyanines containing spherical or cylindrical macrotricyclic moieties.* Polyhedron, 2005. **24**(10): p. 1117-1124.

25. Yılmaz, F., et al., *Catalytic activity of a thermoregulated, phase-separable Pd (II)-perfluoroalkylphthalocyanine complex in an organic/fluorous biphasic system: hydrogenation of olefins.* Catalysis letters, 2009. **130**(3-4): p. 642-647.

26. El-Nahass, M. and K. Abd El-Rahman, *Investigation of electrical conductivity in Schottky-barrier devices based on nickel phthalocyanine thin films.* Journal of alloys and compounds, 2007. **430**(1): p. 194-199.

27. Ho, K.-C. and Y.-H. Tsou, *Chemiresistor-type NO gas sensor based on nickel phthalocyanine thin films.* Sensors and Actuators B: Chemical, 2001. **77**(1): p. 253-259.

28. Liu, C., J. Shih, and Y. Ju, *Surface morphology and gas sensing characteristics of nickel phthalocyanine thin films.* Sensors and Actuators B: Chemical, 2004. **99**(2): p. 344-349.

29. Liu, C.J., J.J. Shih, and Y.H. Ju, *Surface morphology and gas sensing characteristics of nickel phthalocyanine thin films.* Sensors and Actuators B: Chemical, 2004. **99**(2-3): p. 344-349.

30. Jacob, D.S., et al., *Synthesis of one-dimensional structured metal phthalocyanine in an ionic liquid.* Journal of Porphyrins and Phthalocyanines, 2007. **11**(10): p. 713-718.

31. Shah, M., et al., *Investigation of the electrical properties of a surface-type Al/NiPc/Ag Schottky diode using characteristics.* Physica B: Condensed Matter, 2010. **405**(4): p. 1188-1192.

32. Shah, M., et al., *Electrical characterization of the ITO/NiPc/PEDOT: PSS junction diode.* Journal of Physics D: Applied Physics, 2010. **43**(40): p. 405104.

33. Shah, M., et al., *Electrical Characteristics of A1/CNT/NiPc/PEPC/Ag Surface-Type Cell.* Chinese Physics Letters, 2010. **27**(10): p. 106102.

34. Sulaiman, K., et al. *Organic Semiconductors: Applications in Solar Photovoltaic and Sensor Devices*. in *Materials Science Forum*. 2013. Trans Tech Publ.

35. Anthopoulos, T. and T. Shafai, *Effects of temperature on electronic properties of nickel phthalocyanine thin sandwich film structures.* Journal of Vacuum Science & Technology A, 2002. **20**(2): p. 295-298.

36. Anthopoulos, T. and T. Shafai, *Junction properties of nickel phthalocyanine thin sandwich film structures using dissimilar electrodes.* physica status solidi (a), 2001. **186**(1): p. 89-97.

37. Shafai, T. and T. Anthopoulos, *Junction properties of nickel phthalocyanine thin film devices utilising indium injecting electrodes.* Thin Solid Films, 2001. **398**: p. 361-367.

38. Anthopoulos, T. and T. Shafai, *Influence of oxygen doping on the electrical and photovoltaic properties of Schottky type solar cells based on α-nickel phthalocyanine.* Thin Solid Films, 2003. **441**(1): p. 207-213.

39. Narayanan Unni, K. and C. Menon, *Electrical, optical and structural studies on nickel phthalocyanine thin films.* Materials Letters, 2000. **45**(6): p. 326-330.

40. Bayrak, R., et al., *Synthesis, characterization and electrical properties of peripherally tetra-aldazine substituted novel metal free phthalocyanine and its zinc (II) and nickel (II) complexes.* Spectrochimica Acta Part A: Molecular and Biomolecular Spectroscopy, 2013. **105**: p. 550-556.

41. El-Nahass, M., K. Abd-El-Rahman, and A. Darwish, *Fabrication and electrical characterization of p-NiPc/n-Si heterojunction.* Microelectronics journal, 2007. **38**(1): p. 91-95.

42. Neghabi, M., M. Zadsar, and S.M.B. Ghorashi, *Investigation of structural and optoelectronic properties of annealed nickel phthalocyanine thin films.* Materials Science in Semiconductor Processing, 2014. **17**: p. 13-20.

43. Ahmad, Z., S.M. Abdullah, and K. Sulaiman, *Temperature-sensitive chemical cell based on Nickel (II) phthalocyanine-tetrasulfonic acid tetrasodium salt.* Sensors and Actuators A: Physical, 2012. **179**: p. 146-150.

44. Ahmad, Z., et al., *Enhancement of electronic and charge transport properties of NiPc by potassium-tetrasulpho group.* Physica B: Condensed Matter, 2013. **413**: p. 21-23.

45. Sharma, G., et al., *Charge conduction process and photoelectrical properties of Schottky barrier device based on sulphonated nickel phthalocyanine.* Synthetic Metals, 2008. **158**(15): p. 620-629.

46. El-Nahass, M., A. El-Deeb, and F. Abd-El-Salam, *Influence of temperature and frequency on the electrical conductivity and the dielectric properties of nickel phthalocyanine.* Organic electronics, 2006. **7**(5): p. 261-270.

47. Sima, M., I. Enculescu, and M. Sima, *PbSe nanowires grown by the template method.* Optoelectronics And Advanced Materials-Rapid Communications, 2008. **2**(2): p. 67-70.

48. Ohgai, T., et al., *Electrochemical fabrication of metallic nanowires and metal oxide nanopores.* Materials and manufacturing processes, 2007. **22**(4): p. 440-443.

49. Jaleh, B., et al., *Preparation of nickel nanowire within polycarbonate membrane and removing polycarbonate by KrF excimer laser.* Int. J. Phys. Sci, 2011. **6**: p. 4775-4780.

50. Lee, S. and Y. Jun, *Cho SN and Cheon J.* J. Am. Chem. Soc., 2002. **2002**: p. 124.

51. Tao, F., et al., *An Easy Way to Construct an Ordered Array of Nickel Nanotubes: The Triblock-Copolymer-Assisted Hard-Template Method.* Advanced Materials, 2006. **18**(16): p. 2161-2164.

52. Sun, Y., B. Mayers, and Y. Xia, *Metal nanostructures with hollow interiors.* Advanced Materials, 2003. **15**(7-8): p. 641-646.

53. Zhang, M., et al., *Regular Arrays of Copper Wires Formed by Template-Assisted Electrodeposition.* Advanced Materials, 2004. **16**(5): p. 409-413.

54. Nielsch, K., et al., *Uniform nickel deposition into ordered alumina pores by pulsed electrodeposition.* Advanced Materials, 2000. **12**(8): p. 582-586.

55. Pignard, S., et al., *Study of the magnetization reversal in individual nickel nanowires.* Journal of Applied Physics, 2000. **87**(2): p. 824-829.

56. Ertan, A., S.N. Tewari, and O. Talu, *Electrodeposition of nickel nanowires and nanotubes using various templates.* Journal of Experimental Nanoscience, 2008. **3**(4): p. 287-295.

57. Wang, F.-X., Y.-D. Liu, and G.-B. Pan, *Vapor growth and photoconductivity of single-crystal nickel-phthalocyanine nanorods.* Materials Letters, 2011. **65**(5): p. 933-936.

58. Furini, L., et al., *Tuning the nanostructure of DODAB/nickel tetrasulfonated phthalocyanine bilayers in LbL films.* Materials Science and Engineering: C, 2013. **33**(5): p. 2937-2946.

59. Silva, J.R., *Morphological Structure Characterization of PAH/NiTsPc Multilayer Nanostructured Films.* Materials Sciences and Applications, 2011. **02**(11): p. 1661-1666.

60. Kawamori, M., S. Yagi, and E. Matsubara, *Formation of nickel nanowires via electroless deposition under a magnetic field.* Journal of The Electrochemical Society, 2011. **158**(8): p. E79-E83.

61. Farag, A., *Optical absorption studies of copper phthalocyanine thin films.* Optics & Laser Technology, 2007. **39**(4): p. 728-732.

62. Xu, B. and S. Holdcroft, *Molecular control of luminescence from poly (3-hexylthiophenes).* Macromolecules, 1993. **26**(17): p. 4457-4460.

63. Ferrari, A. and J. Robertson, *Interpretation of Raman spectra of disordered and amorphous carbon.* Physical review B, 2000. **61**(20): p. 14095.

64. Fakir, M.S., Z. Ahmad, and K. Sulaiman, *Modification of optical band gap and surface morphology of NiTsPc thin films.* Chinese Physics Letters, 2012. **29**(12): p. 126802.

65. Akin, S. and S. Sönmezoglu, *Nanostructured TiO2 thin films: synthesis and characterisations.* Materials Science and Technology, 2012. **27**(5): p. 342-349.

66. Ghasemi Varnamkhasti, M., et al., *Comparison of metal oxides as anode buffer layer for small molecule organic photovoltaic cells.* Solar Energy Materials and Solar Cells, 2012. **98**: p. 379-384.